Arab J. Nucl. Sci. Appl., Vol. 56, 5, 114-126 (2023)

ISSN 1110-0451

Arab Journal of Nuclear Sciences and Applications

Web site: ajnsa.journals.ekb.eg

(E S N S A)

Radionuclides Determination and Computing Radiobiological Dose for (TENORM) Exposure Using NaI(Tl) Gamma-ray Spectrometer

Fatma Qabeeli[1], Ahmed El-Khatib[1], Mahmoud Abbas[1], Gehad Saleh[2], Mohamed Mitwalli[3,4*]

[(1)]Physics Department, Faculty of Science, Alexandria University, Alexandria 21511, Egypt

[(2)]Nuclear Materials Authority, El-Maadi, P.O. Box 530, Cairo, Egypt

[(3)]Physics Department, Faculty of Science, Mansoura University, Mansoura 35516, Egypt

[(4)]National Network for Nuclear Science, Academy of Scientific Research and Technology, Cairo 11334, Egypt

HIGHLIGHTS

1. NaI(Tl) Gamma-ray spectrometer was employed to determine radionuclides and activity concentration of radioisotopes materialized in younger granites of the El-Missikat area, Central Eastern Desert in Egypt.
2. The detectable radioactivity levels demonstrated peak values of (NORM/TENORM) and contour maps tracked the distribution pattern.
3. The radiological survey of investigated area is crucial, therefore radiobiological impacts were computed and freshened by infographics.

GRAPHICAL ABSTRACT

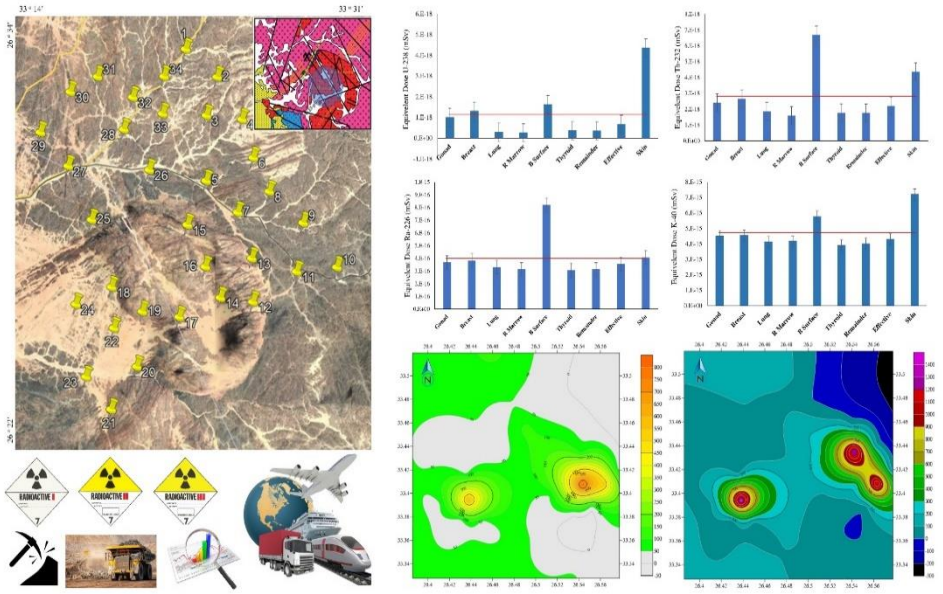

ARTICLE INFO

Article history:

Received: 27th Feb. 2023

Accepted: 10th May 2023

Available online: 15th June 2023

Keywords:

NaI(Tl);
Radiological Protection;
Radioactivity;
Radiation dose;
Gamma-ray spectrometer;
NORM/TENORM.

ABSTRACT

The present study is carried out to determine the natural radioactivity level and assessment of the radiological impact on El-Missikat younger granites of the Central Eastern Desert in Egypt. Regarding the distribution pattern of radionuclides associated with the abundance of naturally occurring and technically enhanced radioactive materials, 34 investigated samples were collected from predetermined locations in the El-Missikat area. The radioanalytical measurements were performed by using NaI(Tl) gamma-ray spectrometer, then PCA3 Oxford software was used to analyze the recorded spectra. The efficiency transfer of Gamma-ray was applied within EFFTRAN software, and the library of radionuclides has been designed to involve radionuclides belonging to the natural uranium-238 and thorium-232 isotopes as well potassium-40. The radiation doses were calculated utilizing activity concentrations and the conversion coefficients recommended by EPA, ICRP, and UNSCEAR. The average values of activity concentrations for U-238, Th-232, and K-40 are (9986.21, 5586.19, and 64.72 Bq/kg) respectively. The average values of calculated effective dose caused by gamma radiation of U-238, Th-232, and K-40 are (6.79E-19, 2.20E-18, and 4.30E-15 Sv/y) respectively. Most of the resulting values are significantly of a high level compared to the worldwide reference EPA, IAEA, ICRP, and UNSCEAR for similar environments. To furnish results regarding radiation protection and human safety integral of organ doses, the excess lifetime cancer risk and hazards indices were calculated to apply a perfect radiation protection methodology for the professionals.

Corresponding author: meto_mms@yahoo.com

DOI: 10.21608/ajnsa.2023.196587.1724

INTRODUCTION

The common radiation exposure is due to environmental radioactivity therefore radioactivity monitoring and radiological protection is associated with naturally occurring and technically enhanced radioactive materials (NORM/TENORM), such as thorium (^{232}Th) and uranium (^{238}U, ^{235}U) decay series in addition to potassium (^{40}K). Special attention to radionuclides production from (^{232}Th, ^{238}U, and ^{235}U) decay series is given to radon, which is considered the main source of natural internal contamination to which occupational and public occupants are exposed [1-7]. The biological effects of the weighting factor denoted; by tissue/organ weighting factors (WT) have been established, which compare the relative biological effects of various types of radiation and the susceptibility of different organs [8-11]. The Environmental Protection Agency (EPA) gives an account of work sponsored by an agency of the United States Government which relies on large-scale data for modeling calculation of equivalent doses based on the radioactivity measurements [12]. The guidance is developed by EPA to provide a common framework to ensure that the regulation of exposure to ionizing radiation is carried out in a consistent and adequately protective manner. This Federal guidance report is designed to provide technical information useful in implementing radiation protection programs. A topic that is currently of great interest is exposure to external radiation from contaminated rocks and sediments, which is the main focus of the calculations used to create EPA reports. The weighting parameters used in federal guidance report No. (11), which were those advised in radiation protection guidelines to federal agencies for occupational exposure have been utilized to calculate the major doses quantity, or effective doses equivalent [12]. The current work is carried out to assess the radioactivity of natural radionuclides using NaI(Tl) gamma-ray spectrometer [13-17]. The activity concentration and its radiological impact will be detected as well as background radioactivity levels that can help protect workers from hazards and monitor the change parallel to the geological process in the area dependent on mining operations and exploration activities in El-Missikat area [18].

GEOLOGY SETTING OF EL-MISSIKAT AREA

El-Missikat area is mainly covered by the neoproterozoic rock units represented by metavolcanics, older granites, and younger granites in addition to felsite dikes, silica, and quartz veins as shown in Fig. (1). El-Missikat has two siliceous veins that are rather large and are located in the middle of the two main shear zones, as seen in Figure (2). The shear zones and these two veins, which crosscut meta-luminous to mildly peraluminous monzogranite, have a general ENE trend and dip between 60^{o} and 70^{o} towards the SS [18, 19]. The siliceous veins generally range in thickness from a few centimeters to over 3.0 meters and are uneven in shape. They also extend for more than 2 kilometers. Light-colored silica, smokey or black silica, and jasperized silica are the three basic varieties that can be identified. White, light grey, and pale brown are only a few of the mild hues that the silica in question exhibits. All of these mentioned types have a normal level of gamma-radioactivity and are microcrystalline or crystalline, not uranium-mineralized. The cryptocrystalline black silica is uranium-mineralized and has a brownish, smoky-to-black tint. The uranium-mineralized jasperized silica is cryptocrystalline, deep red in hue, moderately/high gamma-radioactive, and cryptocrystalline. Brecciation is frequent, and it includes sub-angular pieces of light-colored silica in both the black and jasperized silica [18, 19].

MATERIALS AND EXPERIMENTAL ANALYSIS

Fulfilling the IAEA protocol, TECDOC-1415 [20], involving 34 investigated sample rocks collected from El-Missikat younger granites of Central Eastern Desert in Egypt with an average mass of 0.25 Kg as shown in Fig. (1). The investigated samples were dried in an electric oven at 110°C for 3 h then all samples were ground, and ethanol solution was used for cleaning the grinding bowl to avoid contamination. The grinding process is important to obtain a fine powder that is recommended for gamma-ray efficiency transfer. Sample aliquots were weighted and stored in sealed polyethylene cylindrical containers as the geometric of Ra-226 standard source, with a diameter of 9 cm and height of 3cm. Regarding accurate energy and efficiency calibration of NaI(Tl) gamma-ray spectrometer, NaI(Tl) was used to measure the gamma radioactivity of samples and software of Oxford nuclear measurement

group (PCA3) was used to analyze the recorded spectra. The Oxford Instruments PCA3 is a third-generation multichannel analyzer that plugs into a personal computer and its accompanying software provides a full-featured multichannel analyzer. It contains a 100-MHz Wilkinson analog-to-digital converter (ADC) with a digital spectrum stabilizer (DSS), single channel analyzer (SCA), and multichannel scaler (MCS). The detector specifications resolution of 7.5 % is specified for ^{137}Cs at 661.9 keV gamma line. It is worth noting the NaI crystal is fortified armor bullets of lead within a cupper window 0.5 mm thick, 8.95 g/cm^3 density at room temperature to reduce both of compton effect and specific X-ray. The detection array was energy calibrated using ^{137}Cs (661.9 keV) and ^{60}Co (1173.2 and 1332.5 keV), standard sources in addition to ^{226}Ra standard source.

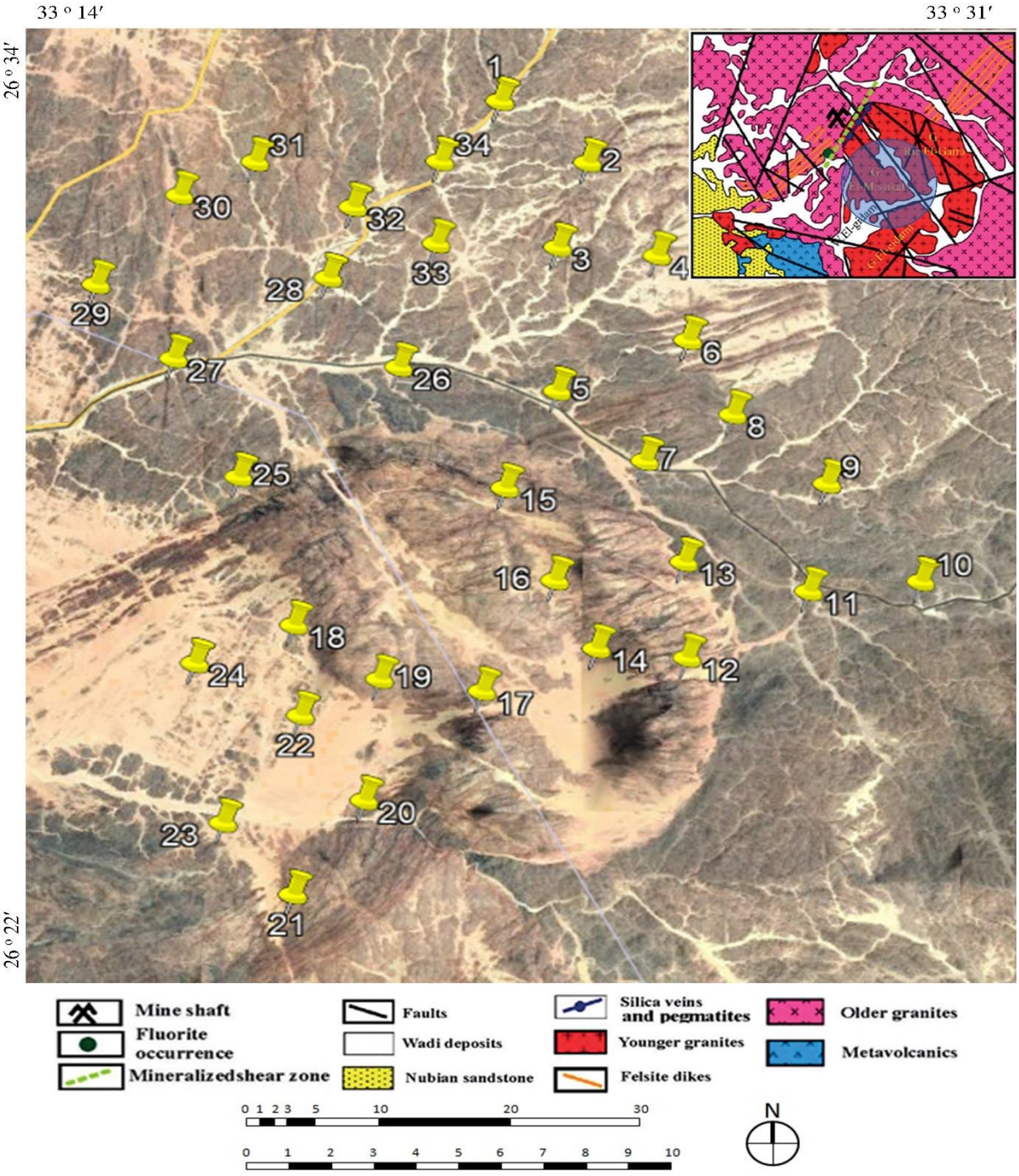

Fig. (1): Map of collected samples, El-Missikat area, Central Eastern Desert, Egypt [18, 19]

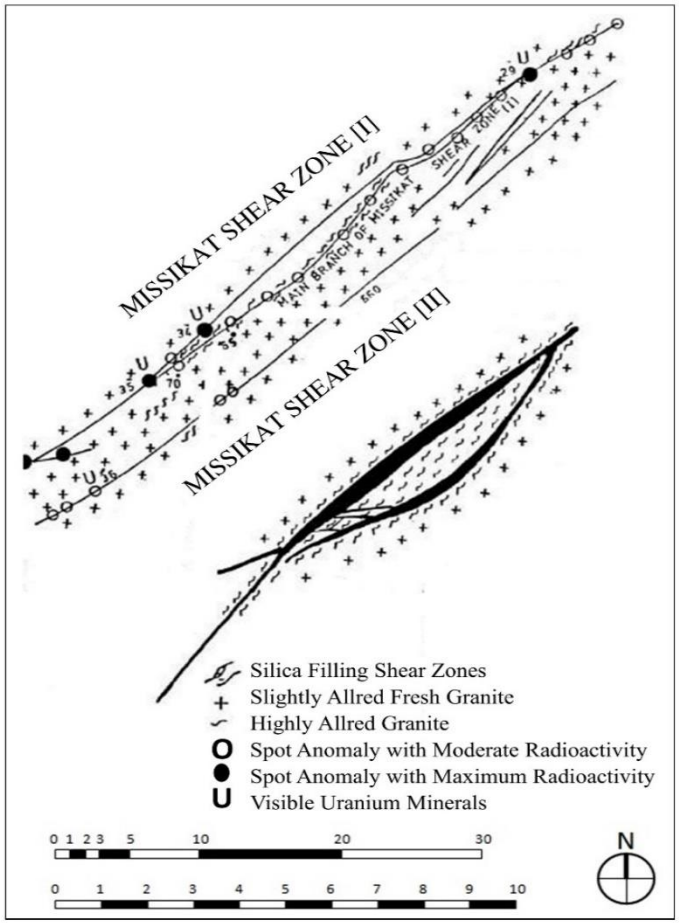

Fig. (2). Sketch showing the two main shear zones of the El-Missikat area within the significant Uranium -occurrence and the siliceous veins (after Abu Dief, 1985) [21].

1. ACTIVITY CONCENTRATION

The natural radionuclide concentrations in the investigated samples were used for uranium, thorium, and potassium to calculate the radiation hazard indicators for humans resulting from continuous exposure to the radiation present in the surrounding environment. The samples' activity concentration A_x was calculated by equation (1). The background is determined where distribution in the environment around the detector, an empty container was counted in the same geometry as the samples. The measurement time of activity or background was 36000 sec [2, 3, 5, 22-24]. The background spectrum was used to correct the net peak area of gamma rays of measured radionuclides. The gamma-emitting nuclides library included the following radionuclides Ra-226, Th-232, and K-40. Total efficiencies transfer corrections have been applied by using EFFTRAN. The recorded spectra of each measured γ-ray energy line were analyzed by PCA3 where ^{214}Pb γ-ray energy peak was estimated at 1120.3 KeV and used to determine the activity concentration of ^{226}Ra. The ^{232}Th radionuclide was estimated from the 911.2 KeV γ-ray energy peak of ^{228}Ac. The ^{40}K radionuclide gamma estimated at the 1461 KeV γ-ray energy peak is used for ^{40}K measurement [8-11].

$$A_x = \frac{Net\ Area}{F\,\varepsilon TM} \qquad \textbf{(1)}$$

where F is the emission probability of the Gamma-ray produced at the energy peak, ε represents the full energy peak efficiency under the given experimental conditions, T corresponds to the measurement time in seconds, and M is the sample mass.

2. CONTENT (PPM)

The contents of the ^{238}U, ^{232}Th, and ^{40}K in (ppm) were calculated using the following equations:

$$PPM = \frac{C_{Ra\text{-}226}\, C_{Th-232}\, C_{K\text{-}40}}{W N_C \ln 2} \qquad \textbf{(2)}$$

where C of ^{226}Ra, ^{232}Th, and ^{40}K radionuclides is activity concentration in (Bq/kg) [3, 4, 8-10, 25-28] and w is the weight factor of the sample. The following expressions directly give content in ppm for ^{226}Ra, ^{232}Th, and ^{40}K, respectively.

^{226}Ra (ppm) = 0.0803 x C (Ra-226)

^{232}Th (ppm) = 0.247 x C (Th-232)

^{40}K (ppm) = 3.862×10^{-3} x C (K-40)

3. HAZARD INDICES (H_{ex})

The external hazard index (H_{ex}) represents the ionization risks of gamma radiation from the environment. The objective is to guarantee that the effective dosage of this radiation does not exceed the allowed limits. Equation (3) yields the external gamma hazard coefficient [2, 3, 5, 6, 12].

$$H_{ex} = \frac{A_K}{4810} + \frac{A_{Th}}{259} + \frac{A_{Ra}}{370} \leq 1 \qquad \textbf{(3)}$$

Indicator of the internal gamma hazards (H_{in}) When short-lived isotopes like radon and thorns produce alpha particles, they are accompanied by gamma rays of varying energy, which are measured by the internal danger index and calculated using equation (4) [2, 3, 5, 6, 12].

$$H_{in} = \frac{A_K}{4810} + \frac{A_{Th}}{259} + \frac{A_{Ra}}{185} \leq 1 \quad \textbf{(4)}$$

In the ideal situation, it is preferred for the H_{ex} and H_{in} to be lower than one in order to have the chance to operate safely for people's radiation protection and their respiratory systems.

4. ACTIVITY UTILIZATION INDEX

To make it easier to compute the dose rates of various mixtures of the radionuclides ^{40}K, ^{232}Th, and ^{226}Ra in the air, the activity utilization index (AUI) is derived. This method is carried out by employing Equation and the conversion factors (f K = 0.041, f Th = 0.604, and f Ra = 0.462). (5) [2, 3, 5, 6, 12].

$$AUI = \frac{A_K}{500} F_K + \frac{A_{Th}}{50} F_{Th} + \frac{A_{Ra}}{50} F_{Ra} \quad \textbf{(5)}$$

5. GAMMA-RAY INDEX

Equation (6) is used to determine the gamma-ray index ($I\gamma$) coefficient, which is used to determine the risk associated with gamma-ray coupled with ^{40}K, ^{232}Th, and ^{226}Ra nuclides The representative values could not exceed 1, which agrees with a conservative, effective dose, and one mSv/y, to ensure the dose rate threshold [2, 3, 5, 6, 12].

$$I\gamma = \frac{A_K}{1500} + \frac{A_{Th}}{100} + \frac{A_{Ra}}{150} \leq 1 \quad \textbf{(6)}$$

6. ALPHA INDEX

The term of alpha index (I_α) refers to an indication that describes the internal risk brought on by the alpha behavior of TENORM radioactivity residues and necessitates alpha index computations. It was proposed to determine the contamination brought on by breathing radon gas (^{222}Rn). Equation (7) is used to calculate the values of the (I_α) [3, 5].

$$I_\alpha = \frac{A_{Ra}}{200} \leq 1 \quad \textbf{(7)}$$

7. EXCESS LIFETIME CANCER RISK

Excess lifetime cancer risk (ELCR) is calculated based on the effective annual dose value by applying the formula used by Equation (8) [2-7, 12, 29].

$$ELCR = DL \times RF \times AED \quad \textbf{(8)}$$

where, in turn, DL, RF, and AEDR stand for, respectively, life expectancy (70 years), risk factor (50 mSv), and effective annual dose rate (Attallah et al., 2020). The chance of developing deadly cancer per Sv disseminated to the general public is indicated as one of the hazard factors.

8. DOSE RATE

Equation (9) is used to determine the dosage rate (AD_γ) from gamma radiation in the air at a height of 1 meter above the ground (UNSCEAR, 2000). As suggested by UNSCEAR and the European Commission, the conversion factors used to convert the activity concentrations (AD_γ) correspond to ^{40}K, ^{232}Th, ^{226}Ra, (0.0417, 0.621, and 0.462) nG/h, respectively [3, 5-7].

$$AD_\gamma = 0.0417 A_K + 0.621 A_{Th} + 0.462 A_{Ra} \quad \textbf{(9)}$$

9. ANNUAL EFFECTIVE DOSE

The activity concentration of investigated samples is employed to calculate the corresponding dose for each body tissue. The effective doses were considered for the human body while applying tissue- coefficients like one unit. The sensitivity of hard/soft tissue varies from one organ to another depending on absorbed rate, hence the equivalent dose is due to different sensitivity and response of organs/tissue, weighting tissue factors are not equal, therefore the AED is calculated by UNSCEAR coefficients. The AED $_{outdoor}$ and AED $_{indoor}$ occupancy factors are (0.2 and 0.8 respectively), The number of hours in a year (8760 h), the absorbed dose AD (nGy/h), and the conversion factor from the AD in the air to the effective dose (0.7 Sv/Gy) are used to compute AED (mSv) [3, 5-7, 30].

$$AED_T = 0.7\ x\ 8760\ x\ ADR\gamma\ x\ 10^{-6} \quad \textbf{(10)}$$

$$AED_{indoor} = 0.8\ x\ 0.7\ x\ 8760\ x\ ADR\gamma\ x\ 10^{-6} \quad \textbf{(11)}$$

$$AED_{outdoor} = 0.2\ x\ 0.7\ x\ 8760\ x\ ADR\gamma\ x\ 10^{-6} \quad \textbf{(12)}$$

As a comparative calculation, the activity concentration of all determined radionuclides and functional coefficients recommended by EPA and the distribution pattern of equivalent dose (nSv/h) are calculated. Table (1) summarizes the radionuclides and their coefficients regarding radioanalytical measurements since annual effective doses were calculated by Equation (13) [12]

$$AED_{organ} = A_n T_f \quad \textbf{(13)}$$

where A_n is the activity concentration of investigated samples (Bq/kg), and T_f define as the coefficient of body hard/soft tissue as shown in (Table 2).

Table (1): The modeling dose coefficients (in Sv/s per Bq/L) recommended by EPA, which were used for the calculation distribution pattern of equivalent dose.

Dose Coefficient (Sv / Bq s m^{-3})									
Nuclide	Gonad	Breast	Lung	R Marrow	B Surface	Thyroid	Remainder	Effective	Skin
U-238	8.19E-22	1.06E-21	2.34E-22	2.18E-22	1.32E-21	2.91E-22	2.86E-22	5.52E-22	3.55E-21
Ra-226	1.76E-19	1.83E-19	1.58E-19	1.50E-19	3.93E-19	1.47E-19	1.50E-19	1.70E-19	1.94E-19
Th-232	3.07E-21	3.38E-21	2.36E-21	2.04E-21	8.51E-21	2.26E-21	2.24E-21	2.79E-21	5.55E-21
K-40	5.84E-18	5.89E-18	5.36E-18	5.40E-18	7.48E-18	5.05E-18	5.19E-18	5.57E-18	9.33E-18

Table (2): The coefficients of body hard/soft tissue recommended by ICRP, which were used for the calculation distribution pattern of equivalent dose.

Tissue/organ	T_f
Stomach, colon, lung, bone marrow	0.12
Gonads	0.20
Urinary bladder, esophagus, liver, glands, and breast	0.05
Bone surface and skin	0.01
Other body organs	0.05

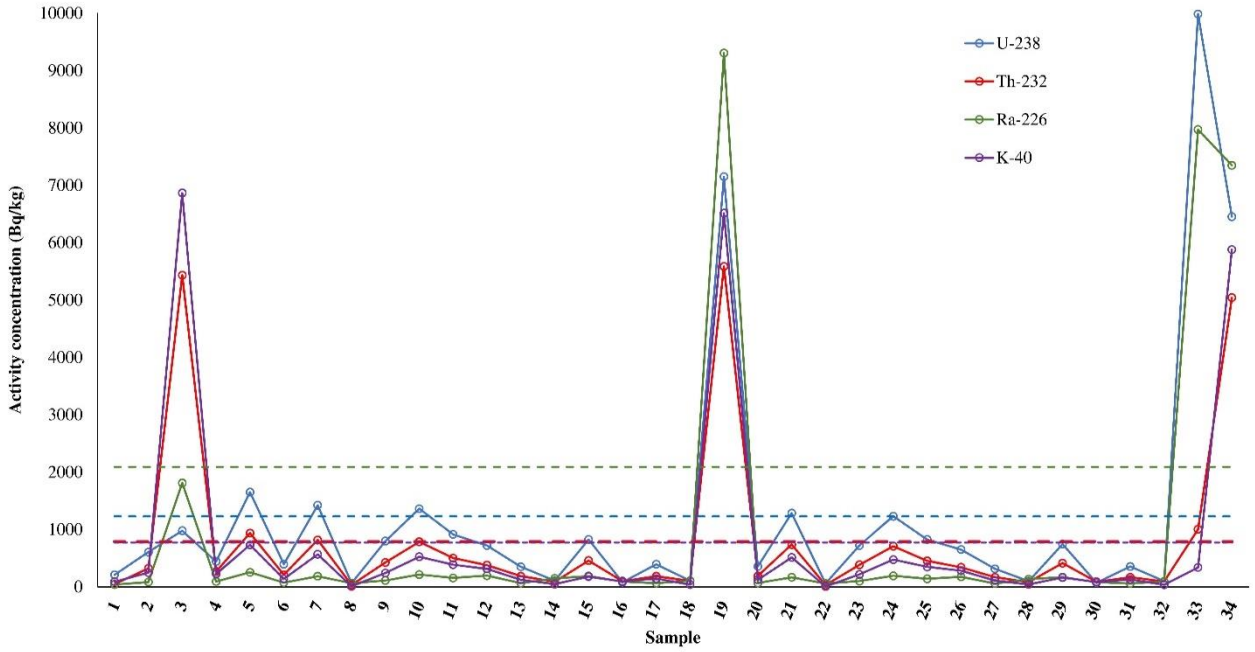

Fig. (3): Comparison of activity concentration (Bq\kg) for each corresponding radionuclide (U-238, Th-232, Ra-226, and K-40) of investigated samples.

RESULTS AND DISCUSSION

The radiometric result of investigated samples is presented in Table (4) and for good discussion, all data of analysis and calculation concerning radiological impact were plotted and furnished in infographics with significates fixed mean values line.

As shown in Fig. (3) the activity concentration of ^{238}U ranged between 57.58 till 9986.21 with an average of 1230.16 Bq/kg, which indicates a high level of radioactivity compared to a natural uranium content range (2.1 and 4.3) mg/kg, since comparison, in Europe, the median uranium content in sediments is estimated to be approximately 2 mg/kg, with a range of variation from less than 1 to more than 90 mg/kg. Regarding ^{238}U the contents of ^{238}U and ^{226}Ra in PPM were calculated and ranged between 3.62 till 838.28 PPM with an average of 99.21 and 79.68 PPM respectively.

As a reference, the average worldwide population-weighted value for ^{226}Ra concentration in terrestrial rocks is 32 Bq/kg [6, 30]. As well for North Africa (Egypt) a reference interval for ^{226}Ra concentration in rocks was found between 5 and 64 Bq/kg with an average value of 17 Bq/kg.

Table (3): The activity concentration (Bq\kg) and the corresponding content (PPM) of investigated samples.

No.	Activity Concentration (Bq\kg)				Content (ppm)			%K
	U-238	Th-232	Ra-226	K-40	eU	eTh	eRa	
1	208.92	46.38	40.18	89.72	16.85	11.42	3.62	0.29
2	605.61	323.26	83.09	247.54	48.84	79.62	7.49	0.79
3	977.96	5432.41	1810.56	6864.72	78.87	1338.03	163.11	21.93
4	442.85	267.39	92.64	224.14	35.71	65.86	8.35	0.72
5	1650.88	936.67	254.15	732.23	133.14	230.71	22.90	2.34
6	394.40	210.51	74.27	137.36	31.81	51.85	6.69	0.44
7	1423.27	817.40	184.09	567.62	114.78	201.33	16.59	1.81
8	63.81	33.95	64.77	7.88	5.15	8.36	5.84	0.03
9	798.22	424.73	110.61	240.71	64.37	104.61	9.96	0.77
10	1363.55	784.99	213.69	524.89	109.96	193.35	19.25	1.68
11	914.78	501.93	155.02	387.06	73.77	123.63	13.97	1.24
12	720.78	377.57	195.33	313.21	58.13	93.00	17.60	1.00
13	349.63	186.61	65.84	121.77	28.20	45.96	5.93	0.39
14	108.13	90.46	147.95	48.49	8.72	22.28	13.33	0.15
15	825.78	458.16	187.60	179.32	66.59	112.85	16.90	0.57
16	78.42	99.51	92.14	90.96	6.32	24.51	8.30	0.29
17	393.68	184.92	64.69	143.82	31.75	45.55	5.83	0.46
18	108.56	103.90	106.95	40.90	8.76	25.59	9.64	0.13
19	7150.19	5586.19	9304.96	6514.56	576.63	1375.91	838.28	20.81
20	355.92	189.97	67.02	123.96	28.70	46.79	6.04	0.40
21	1284.41	737.65	166.13	512.24	103.58	181.69	14.97	1.64
22	57.58	30.63	58.45	7.11	4.64	7.55	5.27	0.02
23	720.35	383.30	99.82	217.23	58.09	94.41	8.99	0.69
24	1230.52	708.41	192.84	473.68	99.24	174.48	17.37	1.51
25	825.54	452.96	139.89	349.30	66.58	111.57	12.60	1.12
26	650.46	340.73	176.28	282.65	52.46	83.92	15.88	0.90
27	315.52	168.41	59.41	109.89	25.44	41.48	5.35	0.35
28	97.58	81.63	133.52	43.76	7.87	20.11	12.03	0.14
29	745.21	413.46	169.30	161.82	60.10	101.84	15.25	0.52
30	70.77	89.81	83.15	82.09	5.71	22.12	7.49	0.26
31	355.27	166.88	58.38	129.79	28.65	41.10	5.26	0.41
32	97.97	93.76	96.52	36.91	7.90	23.09	8.70	0.12
33	9986.21	1002.64	7972.26	338.37	805.34	246.95	718.22	1.08
34	6452.61	5041.20	7348.38	5879.00	520.37	1241.67	662.02	18.78
Max.	9986.21	5586.19	9304.96	6864.72	805.34	1375.91	838.28	21.93
Min.	57.58	30.63	40.18	7.11	4.64	7.55	3.62	0.02
Avg.	1230.16	787.30	884.41	771.31	99.21	193.92	79.68	2.46
St. Dev.	2188.62	1468.15	2344.28	1796.36	176.50	361.61	211.20	5.74
World Avg. [3, 31]	33	45	32	420	2.8	7.4	3.2	1.30

Concerning the activity concentration of ^{232}Th, ^{228}Ac is a decay product of ^{232}Th, therefore its activity concentration in environmental samples should be linked to the level of concentration of it pare, the result of analysis ranged between 519.8 till 11826.9 with an average of 7806.7 Bq/kg and equivalent content ranged between 7.55 till 1375.91 with an average of 193.92 PPM which indicate high radioactivity level as the reference of worldwide average value 45 Bq/kg. Finally, the activity concentration of ^{40}K ranged between 7.11 till 6864.72 with an average value of 771.31 Bq/kg, which is higher than the world average level of 420 Bq/kg [3-5, 32].

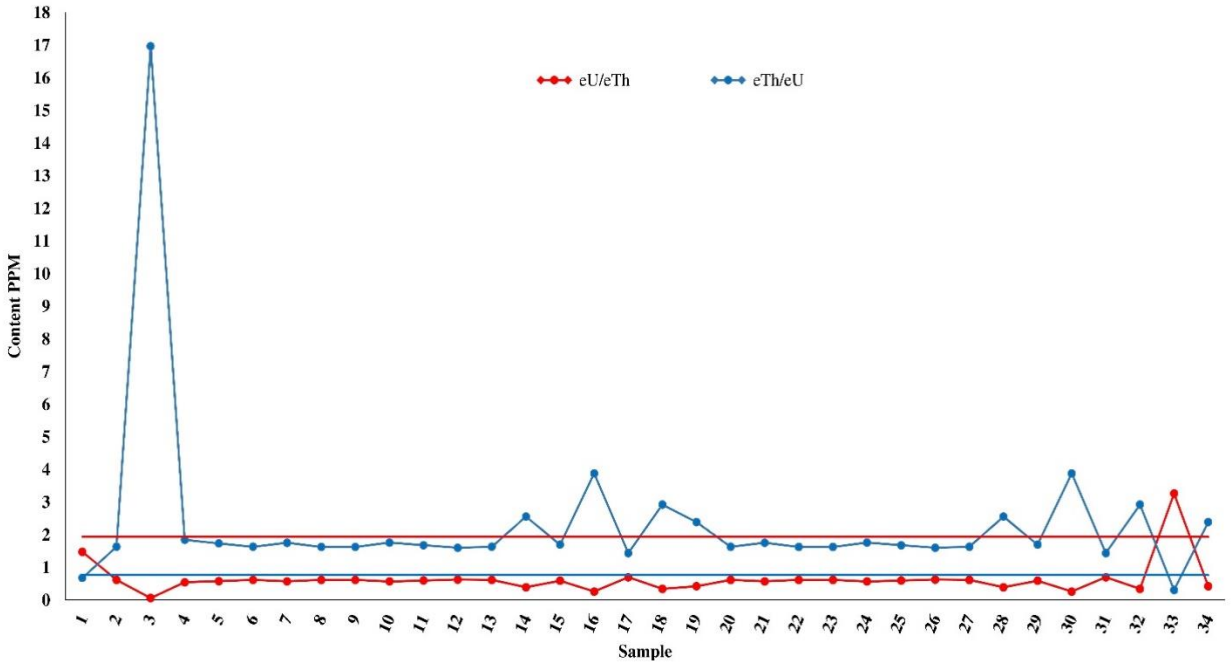

Fig. (4): Comparison of equivalent uranium and thorium ratio (eU/eTh & eTh/eU) PPM for investigated samples.

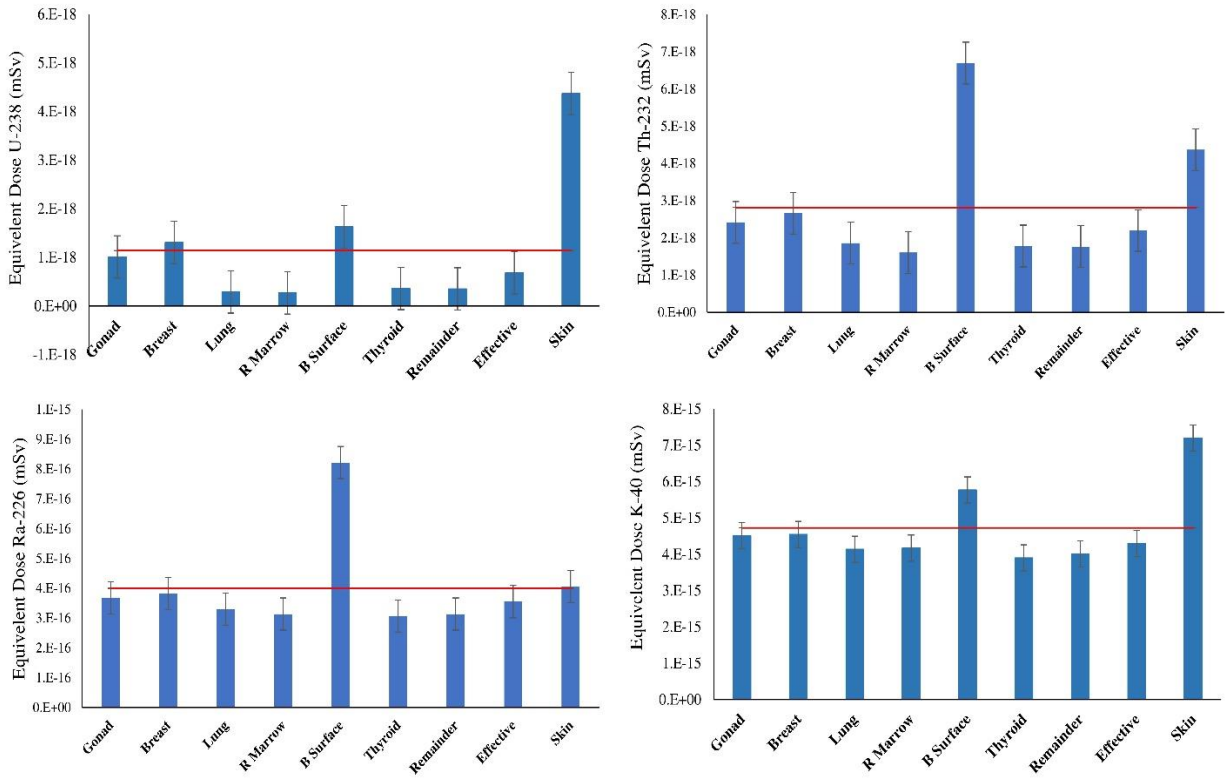

Fig. (5): Comparison of external exposure to radionuclides (U-238, Ra-226, Th-232, and K-40) and distribution pattern of corresponding dose for tissue/organs using EPA modeling dose coefficients.

Table (4): Computing Radiobiological impact of annual Effective Dose, dose rate, hazard indices, and excess lifetime cancer risk.

No.	AED ($mSvy^{-1}$)		AGED	Dose rate	Hazards		AUI	I (ɣ)	I (α)	ELCR
	indoor	outdoor	($mSvy^{-1}$)	($nGyh^{-1}$)	H_{ex}	H_{in}				
1	0.01	0.04	59	9	0.05	0.06	0.94	0.14	0.20	0.000038
2	0.06	0.26	356	53	0.33	0.35	1.34	0.85	0.42	0.000227
3	1.11	4.45	6104	907	5.61	6.05	20.66	14.48	9.05	0.003894
4	0.05	0.22	301	45	0.28	0.30	67.05	0.71	0.46	0.000192
5	0.19	0.76	1036	154	0.95	1.02	5.60	2.46	1.27	0.000661
6	0.04	0.17	238	35	0.22	0.24	12.06	0.56	0.37	0.000152
7	0.16	0.65	893	133	0.82	0.87	4.26	2.13	0.92	0.000570
8	0.01	0.04	53	8	0.05	0.06	10.52	0.12	0.32	0.000034
9	0.09	0.34	468	70	0.43	0.46	1.43	1.11	0.55	0.000299
10	0.16	0.63	868	129	0.80	0.85	7.13	2.06	1.07	0.000554
11	0.10	0.41	560	83	0.52	0.55	10.96	1.33	0.78	0.000357
12	0.08	0.32	443	66	0.41	0.45	7.90	1.05	0.98	0.000283
13	0.04	0.15	211	31	0.19	0.21	5.20	0.50	0.33	0.000134
14	0.02	0.10	134	20	0.12	0.16	3.63	0.31	0.74	0.000086
15	0.10	0.38	524	78	0.48	0.53	2.83	1.24	0.94	0.000334
16	0.02	0.09	128	19	0.12	0.14	6.40	0.30	0.46	0.000082
17	0.04	0.15	209	31	0.19	0.21	1.81	0.49	0.32	0.000133
18	0.02	0.10	137	20	0.12	0.04	3.23	0.32	0.53	0.000087
19	1.52	6.10	8348	1243	7.58	3.37	87.24	19.36	46.52	0.005334
20	0.04	0.16	214	32	0.20	0.02	68.65	0.51	0.34	0.000137
21	0.15	0.59	806	120	0.74	0.06	3.84	1.92	0.83	0.000514
22	0.01	0.03	48	7	0.04	0.02	9.49	0.11	0.29	0.000031
23	0.08	0.31	423	63	0.39	0.04	1.29	1.00	0.50	0.000270
24	0.14	0.57	784	116	0.72	0.07	6.43	1.86	0.96	0.000500
25	0.09	0.37	506	75	0.47	0.05	9.89	1.20	0.70	0.000323
26	0.07	0.29	400	59	0.37	0.07	7.13	0.95	0.88	0.000255
27	0.03	0.14	190	28	0.17	0.02	4.69	0.45	0.30	0.000121
28	0.02	0.09	121	18	0.11	0.05	3.28	0.28	0.67	0.000077
29	0.09	0.34	473	70	0.43	0.06	2.55	1.12	0.85	0.000302
30	0.02	0.08	116	17	0.11	0.03	5.78	0.27	0.42	0.000074
31	0.03	0.14	188	28	0.17	0.02	1.63	0.45	0.29	0.000120
32	0.02	0.09	123	18	0.11	0.03	2.92	0.29	0.48	0.000079
33	0.60	2.38	3252	485	2.89	2.84	74.80	7.26	39.86	0.002083
34	1.32	5.29	7242	1078	6.59	2.67	80.04	16.84	36.74	0.004626
Max	1.52	6.10	8348.13	1242.59	7.58	6.05	87.24	19.36	46.52	0.005334
Min	0.01	0.03	47.82	7.12	0.04	0.02	0.94	0.11	0.20	0.000031
Avg	0.19	0.77	1057.55	157.34	0.96	0.65	15.96	2.47	4.42	0.000675
SD	0.37	1.49	2046.70	304.58	1.86	1.27	25.59	4.76	11.72	0.001307
Limitation [3, 32]		0.05		10			≤ 1			≤ 0.29

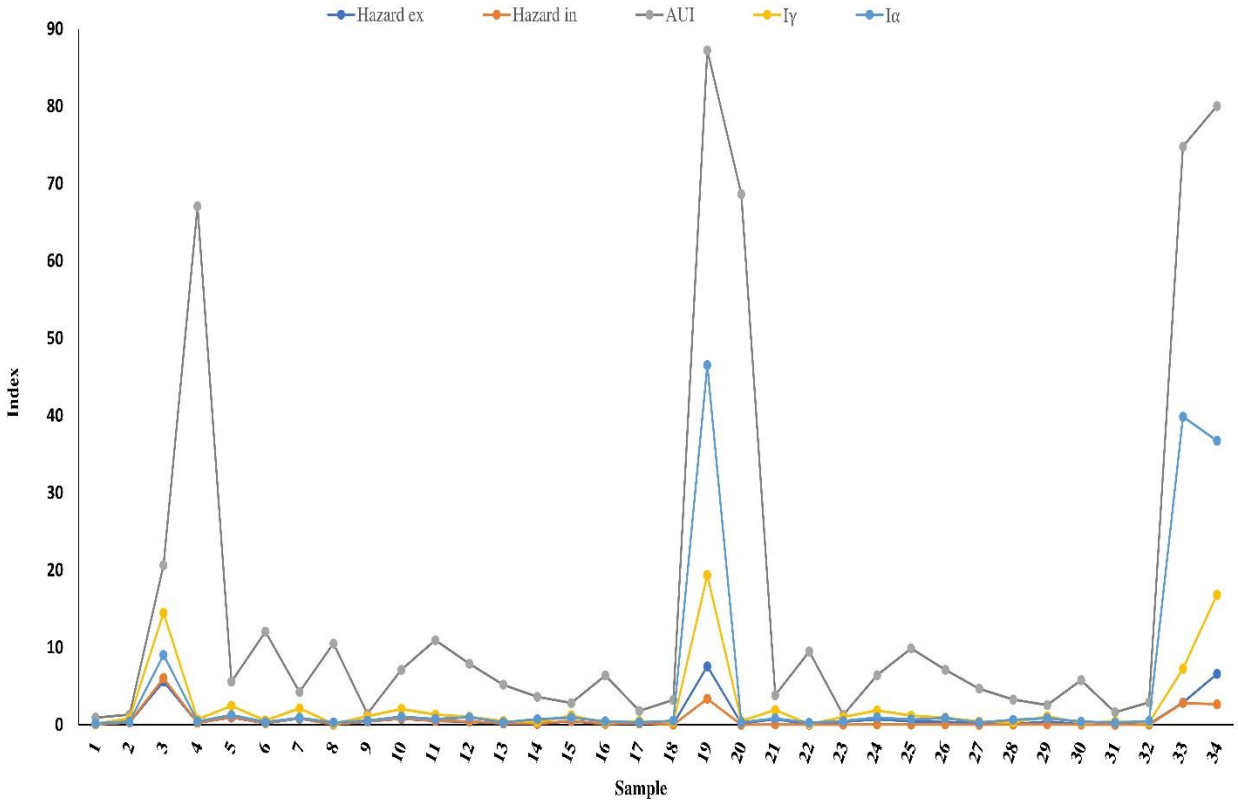

Fig. (6): Comparison of hazard indices for investigated samples.

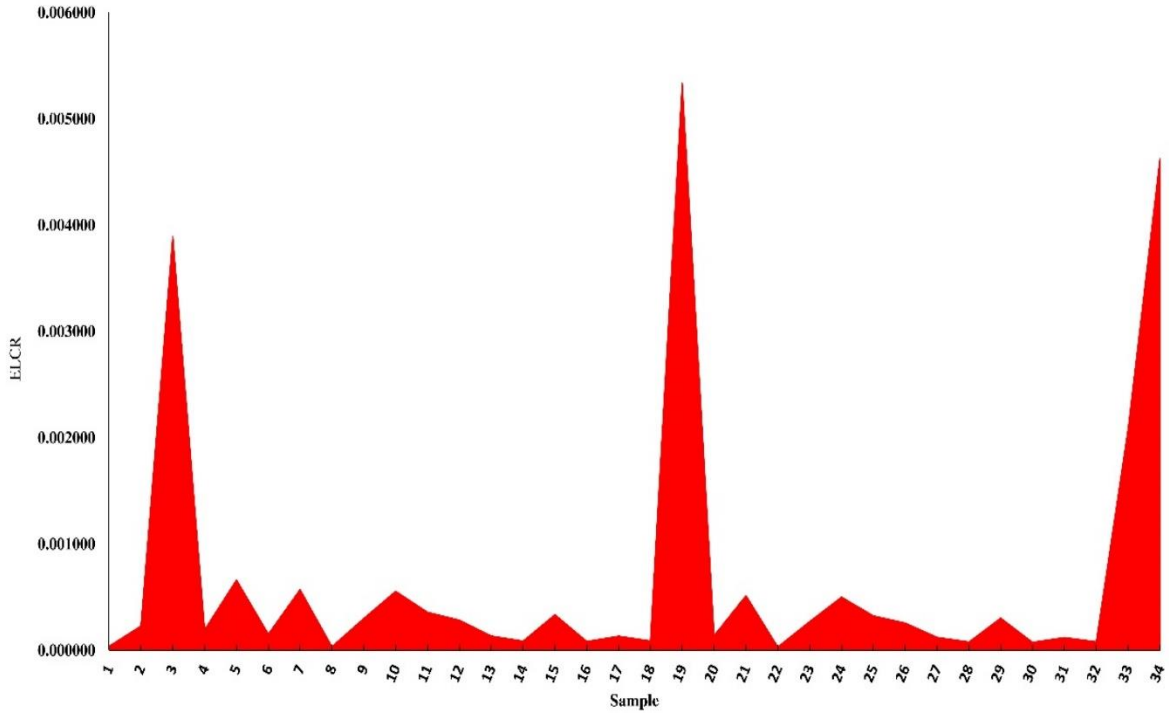

Fig. (7): Comparison of excess lifetime cancer risk estimated from investigated samples.

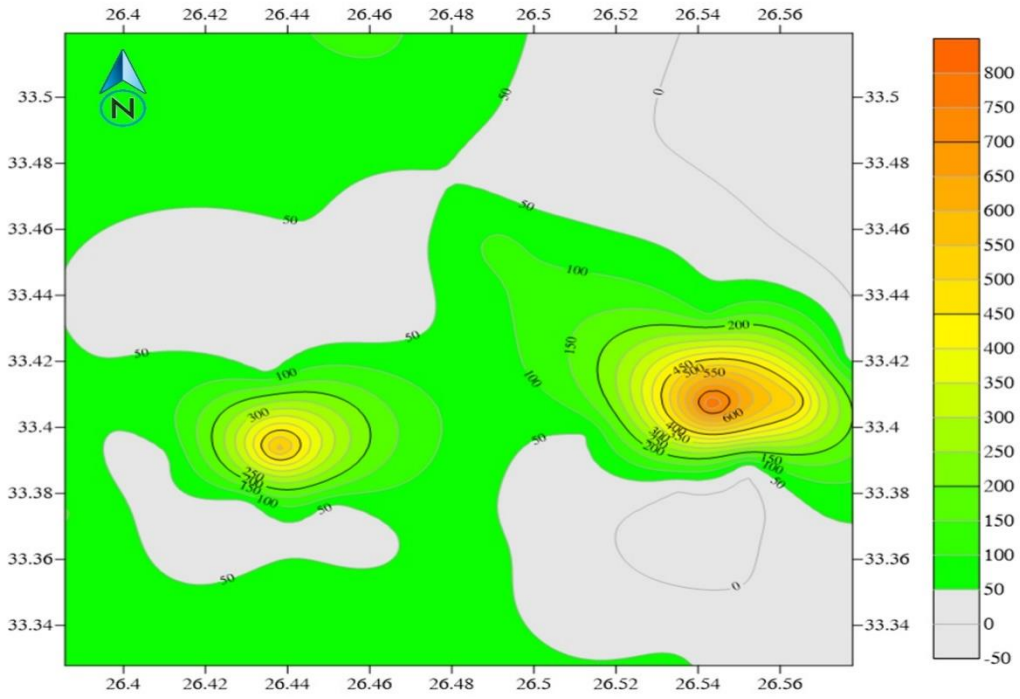

Fig. (8): Contour map for tracking the eU-238 (ppm) for El-Missikat younger granites, Central Eastern Desert, Egypt.

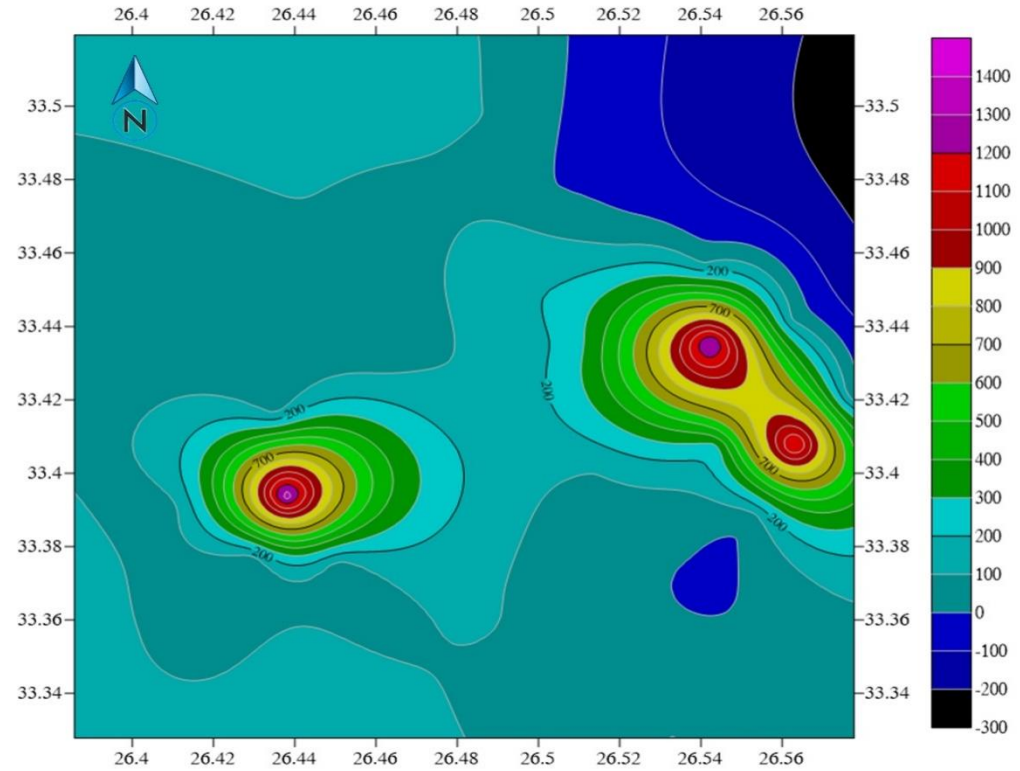

Fig. (9): Contour map for tracking the eTh-232 (ppm) for El-Missikat younger granites, Central Eastern Desert, Egypt.

CONCLUSIONS

According to activity concentration measurements, the distribution pattern of the organs dose was calculated in terms of safety and radiation protection for occupational. The overall effective dose values of the area under study are of significant high radiobiological impact hazards. The calculated effective dose range is (0.01 to 51503.44 with a mean value of 32556.63 and a standard deviation of 21014.28 nSv/h). As well as the calculation property of ELCR helps to apply long-term radiation hazards monitoring to perform good protection protocols for workers from cancer risk. The radiological survey of these places is crucial for determining the radiological social protection under normal conditions and for identifying the areas that may be more contaminated or where radioactive materials may be migrating in or out owing to geological and mining processes. The dataset aid in identifying any fluctuations in the radioisotope background level carried on by geological processes and can be employed as a guide in the Missikate region to identify the presence of dangerous radiation that might endanger individual and occupational.

REFERENCES

[1] Dragović, S. and A. Onjia, *Classification of soil samples according to their geographic origin using gamma-ray spectrometry and principal component analysis.* Journal of Environmental Radioactivity, 2006. **89**(2): p. 150-158.

[2] IAEA, *Soil Sampling for Environmental Contaminants*. 2004, Vienna: International Atomic Energy Agency.

[3] IAEA, *Analytical Methodology for the Determination of Radium Isotopes in Environmental Samples*. 2011, Vienna: International Atomic Energy Agency.

[4] IAEA, *Nuclear Data for the Production of Therapeutic Radionuclides*. 2012, Vienna: International Atomic Energy Agency.

[5] IRSN, *Natural Uranium and the environment: appendices*, B. Bonin, Editor. 2012, nstitut de radioprotection et de sûreté nucléaire.

[6] UNSCEAR, *Sources and Effects of Ionizing Radiation*, ed. R.t.t.G. Assembly. Vol. 1. 2000, New York: United Nations Scientific Committee on the Effects of Atomic Radiation.

[7] UNSCEAR, *Report of the United Nations Scientific Committee on the Effects of Atomic Radiation* UNSCEAR, 2011. **58**: p. 12.

[8] Mitwalli, M., et al., *Environmental Radioactivity Monitoring Using High Resolution Gamma-ray Spectrometer for Lake Manzala in Egypt.* Arab Journal of Nuclear Sciences and Applications, 2022. **55**(4): p. 139-149.

[9] Saleh, G.M., et al., *Environmental Radioactivity of Radon and its Hazards in Hamash Gold Mine, Egypt.* Arab Journal of Nuclear Sciences and Applications, 2019. **52**(4): p. 190-196.

[10] MITWALLI, M., et al., *Radon Measurement and Radiological Dose Assessment From Terrestrial Rocks Using Solid-State Nuclear Track Detectors.* Arab Journal of Nuclear Sciences and Applications, 2022: p. 1-8.

[11] MITWALLI, M., et al., *Evaluation of Radon Radioactivity and Radiological Impact by Using Solid-State Nuclear Track Detector for Erediya younger granites of Central Eastern Desert in Egypt.* Arab Journal of Nuclear Sciences and Applications, 2023: p. -.

[12] EPA, *External Exposure to Radionuclides in Air, Water, and Soil*, in *EPA Federal Guidance Report*. 1993, Environmental Protection Agency: Washington. p. 238.

[13] Casanovas, R., J. Morant, and M. Salvadó, *Implementation of gamma-ray spectrometry in two real-time water monitors using NaI (Tl) scintillation detectors.* Applied Radiation and Isotopes, 2013. **80**: p. 49-55.

[14] Avwiri, G. and S. Olatubosun, *Assessment of environmental radioactivity in selected dumpsites in Port Harcourt, Rivers State, Nigeria.* International Journal of Scientific & Technology Research, 2014. **3**(4): p. 283-269.

[15] Senthilkumar, G., et al., *Natural radioactivity measurement and evaluation of radiological hazards in some commercial flooring materials used in Thiruvannamalai, Tamilnadu, India.* Journal of Radiation Research and Applied Sciences, 2014. **7**(1): p. 116-122.

[16] Obaid, S.S., D. Gaikwad, and P. Pawar, *Determination of natural radioactivity and hazard in some rock samples.* Bionano Frontier, 2015. **8**(3): p. 125-127.

[17] Wang, J., et al., *Automated spectra analysis of in situ radioactivity measurements in the marine environment using NaI (Tl) detector.* Applied Radiation and Isotopes, 2018. **141**: p. 88-94.

[18] Abu-Deif, A., *Geology of uranium mineralization in EL Missikat area, Qena-Safaga road, Eastern Desert, Egypt.* Unpublished M. Sc. thesis, Al-Azhar University, 1985.

[19] Ibrahim, A.E.-L.A., et al., *Geological and geochemical studies on El-Missikat granites, Central Eastern Desert, Egypt.* Известия Уральского государственного горного университета, 2020(4 (60)): p. 7-18.

[20] IAEA, *Soil Sampling for Environmental Contaminants*. IAEA TECDOC Series. 2004, Vienna: International Atomic Energy Agency.

[21] Bakhit, F., H. Assaf, and A.A. DIEF, *Correlation study on the geology and radioactivity of surface and subsurface working at El Missikat area, Central Eastern Desert, Egypt.* Mining Geology, 1985. **35**(193): p. 345-354.

[22] Abbas, Y.M., et al., *Measurement of 226Ra concentration and radon exhalation rate in rock samples from Al-Qusair area using CR-39.* Journal of Radiation Research and Applied Sciences, 2020. **13**(1): p. 102-110.

[23] Lakehal, C., M. Ramdhane, and A. Boucenna, *Natural radionuclide concentrations in two phosphate ores of east Algeria.* Journal of environmental radioactivity, 2010. **101**(5): p. 377-379.

[24] Lawrie, W., et al., *Determination of radium-226 in environmental and personal monitoring samples.* Applied Radiation and Isotopes, 2000. **53**(1-2): p. 133-137.

[25] Barooah, D. and P.P. Gogoi, *Study of radium content, radon exhalation rates and radiation doses in solid samples in coal-mining areas of Assam and Nagaland using LR-115 (II) nuclear track detectors*. 2019, India: Vishal Publishing Company.

[26] El-Farrash, A.H., H.A. Yousef, and A.F. Hafez, *Activity concentrations of 238U and 232Th in some soil and fertilizer samples using passive and active techniques.* Radiation Measurements, 2012. **47**(8): p. 644-648.

[27] Grossi, C., et al., *Inter-comparison of different direct and indirect methods to determine radon flux from soil.* Radiation Measurements, 2011. **46**(1): p. 112-118.

[28] Hashim, A.K. and L.A. Najam, *Measurement of uranium concentrations, radium content and radon exhalation rate in iraqian building materials samples.* International Journal of Physics, 2015. **3**(4): p. 159-164.

[29] Kathren, R.L., *Radioactivity in the environment : sources, distribution, and surveillance*. 1984: Harwood Academic Publishers.

[30] ICRP, *Human Respiratory Tract Model for Radiological Protection*, I.P. 66, Editor. 1994, ICRP.

[31] UNSCEAR, U., *Sources and effects of ionizing radiation.* United Nations Scientific Committee on the Effects of Atomic Radiation, 2000.

[32] El-Taher, A., *Terrestrial gamma radioactivity levels and their corresponding extent exposure of environmental samples from Wadi El Assuity protective area, Assuit, Upper Egypt.* Radiation protection dosimetry, 2011. **145**(4): p. 405-410.